

Enhanced Robustness in Integrated Structural/Control Systems Design

Ramana V. Grandhi* and Iftikhar Haq†
Wright State University, Dayton, Ohio 45435
and

N. S. Khot‡
Wright Laboratory, Wright-Patterson Air Force Base, Ohio 45433

This paper addresses maximizing the robustness of an integrated structural/control system for increasing the stability margin under parametric uncertainties. The robustness limit is defined for a linear time-invariant system consisting of structured perturbations. The optimization problem has considered the closed-loop eigenvalues, damping parameter, and robustness as design constraints. Effects of increasing the stability robustness of a closed-loop system are demonstrated on two structural optimization examples.

Introduction

RECENTLY, the simultaneous design of space structures and their control systems has received tremendous attention due to the reductions realized in structural weights, control efforts, and improvements in closed-loop performance. This integrated design approach modifies both the structural properties and the control system characteristics in an optimal way to meet the stringent space structure requirements. Some of the recent efforts on the integrated design approach are given in Refs. 1-6. The integrated optimization problems included design constraints on transient response, actuator forces, nonstructural mass locations and magnitudes, closed-loop eigenvalues, and damping parameters.

In designing a control system, a nominal model is selected and a controller is designed for it. The resulting control system may or may not be stable with respect to the presence of parametric uncertainties in the physical model. It is desirable to determine to what extent a nominal system remains stable when it is subjected to a certain class of perturbations. This measure is called the stability robustness bound. This paper concentrates on improving the stability robustness bound of the integrated structural/control system for model uncertainties. From the control system point of view, the stability robustness analysis problem has been investigated by many researchers. The uncertainties present in the model are classified into two types; namely, structured and unstructured perturbations. These include disturbances as well as parameter variations. In the unstructured perturbation model, only an upper bound on the norm of perturbed matrix is assumed known. In the case of structured perturbations, the knowledge about the location of uncertainties and/or relative magnitude bound is available. Additionally, these perturbations can be time-invariant or time-dependent. Methods are being developed for both frequency domain analysis and time-domain analysis. In the following, some of the representative papers in the time domain for state-space models are referenced.

Patel et al.⁷ and Patel and Toda⁸ developed quantitative measures on time-varying nonlinear perturbation of an asymptotically stable linear system. They derived expressions for bounds on unstructured and structured perturbations. A less conservative bound on the linear perturbations of similar systems was obtained by Yedavalli et al.^{9,10} by developing an improved structured perturbation model. In this model, the authors provided more information on the nature of uncertainties by identifying the location of perturbations. The aforementioned time-domain criteria presented in Refs. 7-10 solve a certain Lyapunov equation for stability robustness. Hence, implicit in all their results is some conservativeness in determining the upper bounds of the parameter variations. Juang et al.¹¹ and Qiu and Davison¹² independently developed a robustness bound for an asymptotically stable linear time-invariant system. Their approach is based on the spectral radius of a perturbed system matrix. The method aims at finding a critical frequency that maximizes the spectral radius. The authors tried to reduce the conservativeness of the bound by not solving the Lyapunov equation. The present research work utilizes methods given in Refs. 11 and 12 in improving the robustness bound of the integrated structural/control system.

Lim and Junkins¹³ carried robustness optimization by using the Patel and Toda⁸ approach and also minimized the eigenvalue sensitivity for improving the stability robustness. The authors concluded that maximization of the stability robustness measure produces more robust designs than minimizing the eigenvalue sensitivity measures. Rew et al.¹⁴ presented a pole placement technique for obtaining a robust eigenstructure using the state energy, control energy, and stability robustness measure (condition number of the closed-loop eigenvectors) as the objective functions. A least squares approach was used in determining the well-conditioned eigenvectors. Similar studies were conducted by Juang et al.¹⁵

In this paper, the integrated design is accomplished by imposing constraints on the robustness bound, closed-loop damping parameter, and the imaginary part of the closed-loop eigenvalues of the active control system. The mathematical optimization problem is solved by using the NEWSUMT-A program. A two-bar truss and an ACOSS-FOUR model are selected for the numerical studies. Simplifications identified in robustness measure calculations and their advantages in the optimization scheme are demonstrated.

Dynamic Analysis

The state-space equation describing the dynamic behavior of a structure is given as

$$\dot{x} = Ax + Bf \quad (1)$$

Presented as Paper 90-1059 at the AIAA/ASME/ASCE/AHS/ACS 31st Structures, Structural Dynamics and Materials Conference, Long Beach, CA, April 2-4, 1990; received May 7, 1990; revision received Aug. 20, 1990; accepted for publication Aug. 29, 1990. This paper is declared a work of the U.S. Government and is not subject to copyright protection in the United States.

*Associate Professor, Department of Mechanical and Materials Engineering. Member AIAA.

†Graduate Research Assistant, Department of Mechanical and Materials Engineering. Member AIAA.

‡Aerospace Engineer. Member AIAA.

where $x(t)$ is the state variable vector and $f(t)$ is the control input vector. In Eq. (1), A and B are the plant and input matrices, and the detailed derivations of these matrices can be found in Ref. 6.

Equation (1) is known as the state input equation. The state output equation is given as

$$y = Cx \quad (2)$$

where y is an output vector, and C is the output matrix that would be equal to B' if the actuators and sensors are collocated. In order to design a linear quadratic regulator, a performance index J is defined as

$$J = \int_0^t (x'Qx + f'Rf) dt \quad (3)$$

where Q and R are the state and control energy weighting matrices that have to be positive semidefinite and positive definite, respectively. The result of minimizing the quadratic performance index and satisfying the state input equation gives the optimal control system as

$$\dot{x} = A_{cl}x \quad (4)$$

The complex eigenvalues of the closed-loop matrix A_{cl} can be written as

$$\lambda_i = \bar{\sigma}_i \pm j\bar{\omega}_i \quad (5)$$

and the damping factor ξ_i is given by

$$\xi_i = -\frac{\bar{\sigma}_i}{(\bar{\sigma}_i^2 + \bar{\omega}_i^2)^{1/2}} \quad (6)$$

Robustness Measure

The linear time-invariant model of the physical system is described by the following equation with linear time-invariant perturbations

$$\dot{x} = (A_{cl} + \Delta A_{cl})x \quad (7)$$

where ΔA_{cl} is the perturbation of A_{cl} matrix.

In Ref. 16 several robustness definitions were compared for aerospace structural models and a suitable method was identified for design optimization studies. Based on these comparisons, a robustness bound defined by Juang et al.¹¹ and Qiu and Davison¹² was used in this work for structured perturbations. (The locations of the A_{cl} matrix uncertainties are known.) According to their definition, the perturbed system [Eq. (7)] is stable if

$$|\Delta A_{cl}| \leq \mu_e \cdot U_e \quad (8)$$

$$\mu_e < \frac{1}{\sup \rho[D(p > 0) \cdot U_e]} = \mu_{JQ} \quad (9)$$

where

$$D(p) = |(jpI - A_{cl})^{-1}|$$

p = operating frequency

\sup = supremum over a range of p

$\rho[\]$ = Spectral radius of $\[\]$

μ_{JQ} = Robustness measure of Juang et al.¹¹ and Qiu and Davison¹²

U_e = perturbation identification matrix¹⁰

The matrix U_e provides information on the structure of perturbations. The elements of U_e may vary between 0 and 1. If the perturbations in $A_{cl}(i, j)$ are known to be zero, then $U_e(i, j) = 0$. If sufficient knowledge of perturbations is not

known, then the corresponding elements of U_e can be assigned a value of 1. However, a U_e matrix with all elements equal to 1 would give conservative results. In Refs. 11 and 12, U_e was formed using the following expression in order to reduce the conservativeness of the robustness bound.

$$U_e(i, j) = \frac{|A_{cl}(i, j)|}{\max_{i,j} |A_{cl}(i, j)|} \quad (10)$$

In this work, this definition has been used for U_e .

Robustness Calculation—Implementation

First the closed-loop matrix A_{cl} is computed using the optimal control theory. The spectral radius ρ is calculated for the matrix given in the denominator of Eq. (9) by finding its eigenvalues and taking their moduli. The spectral radius is equal to the maximum of these values for a selected p value. For each value of p , one spectral radius value is computed, and the robustness measure is evaluated by varying p ($p > 0$) up to a very large value in small increments of p . The maximum spectral radius value among all these numbers gives the inverse of robustness. To identify which p value gives the maximum spectral radius, one has to conduct a large number of matrix inversions, multiplications, and eigenvalue extractions. The whole methodology is computationally intensive during the design optimization phase due to the iterative nature of the procedure. Based on the example problems, this research work has resulted in a simplified approach in identifying the spectral radius local maxima locations. Instead of varying p from 0 to ∞ , the spectral radius is computed only at the closed-loop matrix eigenvalues. The local maxima occurred at the magnitudes of the closed-loop eigenvalues for the problems addressed in this work. This observation was validated on two truss structure examples. In this work, the variable p is called the operating frequency, and the p value corresponding to the maximum spectral radius is called the critical operating frequency.

The two-bar truss shown in Fig. 1 is used as the first example. Details of the optimum gain matrix and the closed-loop eigenvalues are given in Ref. 16 for one of the configurations. The spectral radius plot with the operating frequency is shown in Fig. 2. The magnitudes of the closed-loop eigenvalues are 52.8 and 235.8, and it can be seen from Fig. 2 that the local peaks occur at these values. Because it is a two-degree-of-freedom system, there are a maximum of two local peaks in ρ at the closed-loop eigenvalue locations. Everywhere else, ρ value is smaller than the maximum peak value. The robustness value, which is the inverse of the spectral radius, corresponds to the global maximum of the spectral radius. Figure 3 shows the variation of the critical operating frequency with the cross-sectional areas. Both the cross-sectional areas are changed simultaneously. The maximum spectral radius occurs at the second closed-loop eigenvalue at the beginning and then switches to the first eigenvalue. Both eigenvalues are plotted with the cross-sectional area changes. The critical operating frequency

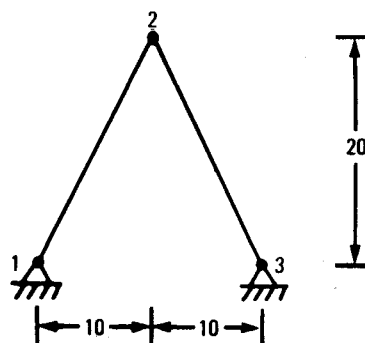


Fig. 1 Two-bar truss.

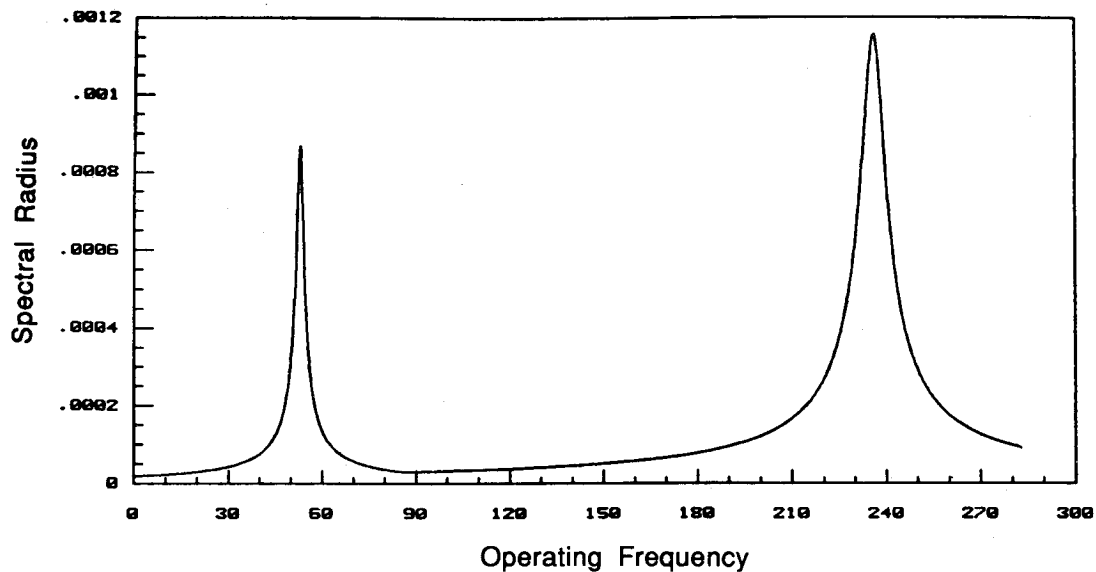


Fig. 2 Two-bar truss spectral radius with operating frequency.

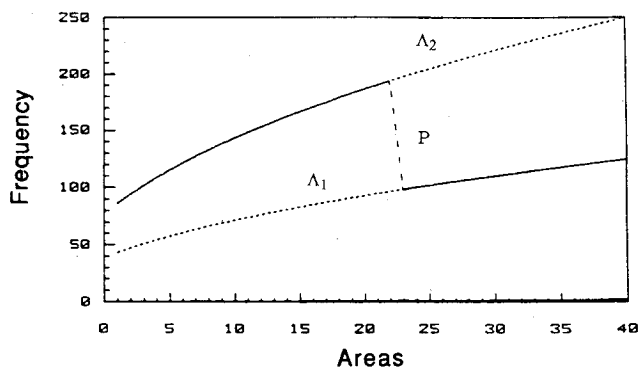


Fig. 3 Two-bar truss operating frequency with areas.

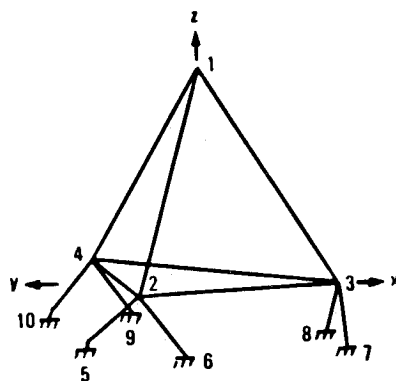


Fig. 4 ACOSS-FOUR model.

is represented as a solid line, and the system eigenvalues are represented as dotted lines. The spectral radius calculation concept is validated also for the ACOSS-FOUR structure shown in Fig. 4. The magnitudes of the closed-loop eigenvalues are 1.34, 1.67, 2.89, 2.96, 3.4, 4.21, 4.66, 4.76, 8.54, 9.25, 10.29, and 12.90. The peaks corresponding to the closed-loop eigenvalue magnitudes are shown in Fig. 5.

This observation has a profound effect in the integrated optimization, due to a much reduced number of matrix operations at each analysis step. So, in this work the robustness bound is evaluated by computing the spectral radii just at the closed-loop eigenvalues.

Numerical Studies

The robustness improvement studies were performed on two structures described in Refs. 2 and 6. Both structures were

Table 1 Two-bar truss robustness design studies

Function	Initial design	Case I.1	Case I.2
Weight	44.72	6.90	10.75
Robustness	1.790	0.626	0.835
$\xi_1 \geq 0.029$	0.056	0.169	0.118
$\bar{\omega}_1 \geq 1.174$	2.987	1.174	1.460
X_1	1000.0	154.8	254.8
X_2	1000.0	154.0	226.0

Table 2 ACOSS-Four robustness design studies

Function	Initial design	Case II.1	Case II.2	Case II.3
Weight	43.70	18.56	19.24	21.28
Robustness	1.06	1.69	1.86	2.21
$\xi_1 \geq 0.15$	0.055	0.15	0.15	0.15
$\bar{\omega}_1 \geq 1.341$	1.341	1.341	1.341	1.341
$\bar{\omega}_2 \geq 1.6$	1.66	1.60	1.60	1.60
X_1	1000.0	182.9	186.6	189.0
X_2	1000.0	231.2	273.8	330.3
X_3	100.0	302.3	316.0	395.5
X_4	100.0	276.6	281.2	313.2
X_5	1000.0	332.7	355.9	327.4
X_6	1000.0	228.3	222.4	241.3
X_7	100.0	252.2	255.7	350.8
X_8	100.0	198.0	281.8	334.7
X_9	100.0	206.6	87.2	48.6
X_{10}	100.0	213.4	193.8	214.6
X_{11}	100.0	29.7	29.8	30.4
X_{12}	100.0	168.0	169.3	192.0

designed with and without the robustness constraint. The optimization problem was solved by using the NEWSUMT-A¹⁷ computer program. This algorithm is based on quadratic extended interior penalty function method with modified Newton's method of unconstrained minimization.

Two-Bar Truss

The two-bar truss shown in Fig. 1 was selected for its simplicity in doing several parametric studies. A nonstructural mass of two units was attached at node two. The structural dimensions were specified in nondimensional units. The weighting matrices Q and R were taken as identity matrices in calculating the A_{cl} matrix. Figure 6 shows the variation of the robustness with the cross-sectional areas. The robustness value increases with an increase in the cross-sectional areas.

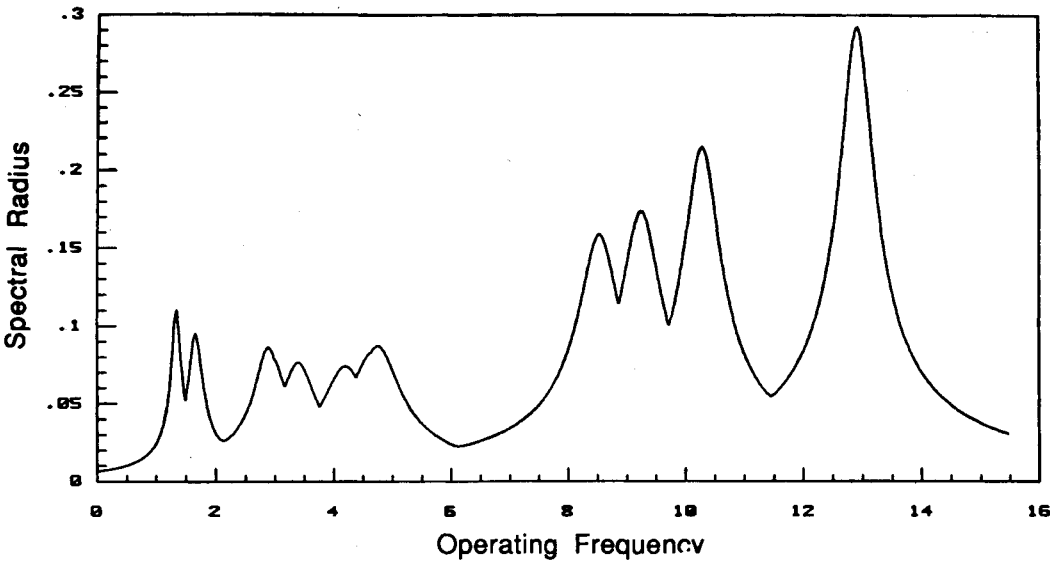


Fig. 5 ACOSS-FOUR truss spectral radius.

Table 3 ACOSS-Four closed-loop systems comparison				
Function	Initial design	Case II.1	Case II.2	Case II.3
Min $\tilde{\omega}$	1.34	1.34	1.34	1.34
Max $\tilde{\omega}$	12.90	7.74	7.97	8.57
Min ξ	0.006	0.031	0.035	0.036
Max ξ	0.055	0.15	0.15	0.15
P.I. ^a (<i>J</i>)	764.4	117.8	135.8	153.3
Control effort	78.6	27.9	32.3	38.1

^aPerformance Index.

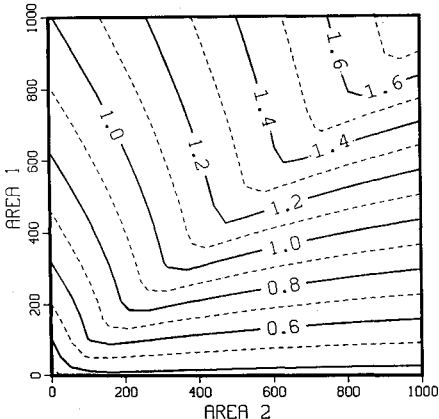


Fig. 6 Two-bar truss robustness variation with areas.

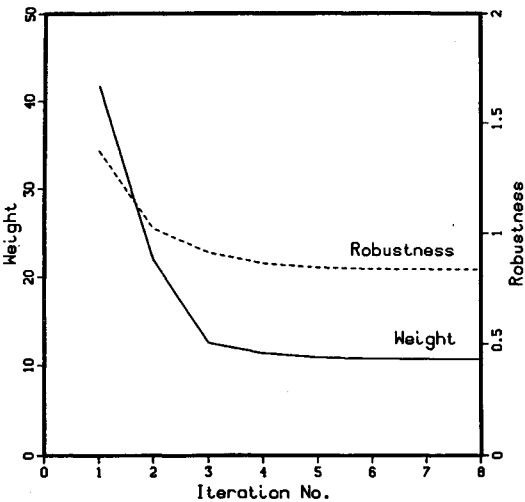


Fig. 7 Two-bar truss design iteration history.

The following optimization problem was solved first. Minimize the structural weight subject to

$$\tilde{\omega}_1 \geq 1.174$$
$$\xi_1 \geq 0.029$$
$$X_i \geq 10.0, \quad i = 1, 2$$

where X_i is the i th design variable.

The optimum results are presented as case I.1 in Table 1. The structural weight was minimized from 44.72 to 6.9 units, the eigenvalue constraint was active at the optimum, and the robustness value was 0.626. The optimum solution very much depends on whether the constraints were posed as equality or inequality constraints. The optimum solution for equality constraints has a much larger structural weight because of the additional restrictions imposed on the search domain. In case I.2, an additional constraint on robustness bound was imposed to increase the previous robustness by 33%. Results are presented in Table 1 with the complete details and Figure 7 shows the variation of structural weight and robustness bound with the optimization iterations. The robustness bound decreased with the decrease in structural weight. A 33% increase in the robustness was accomplished with a weight penalty of more than 50%. Figure 8 shows the variation of the optimum weight with percentage improvement in robustness. The structural

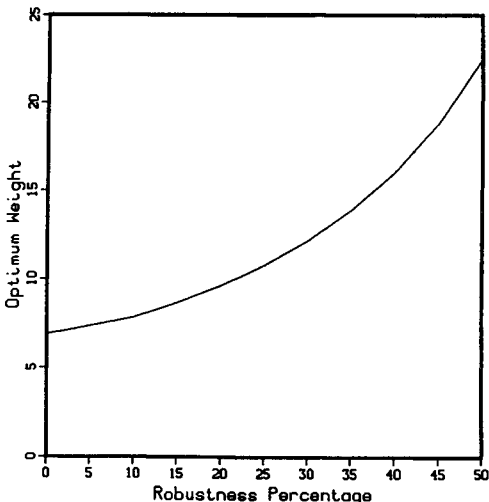


Fig. 8 Two-bar truss optimum weight vs robustness improvement.

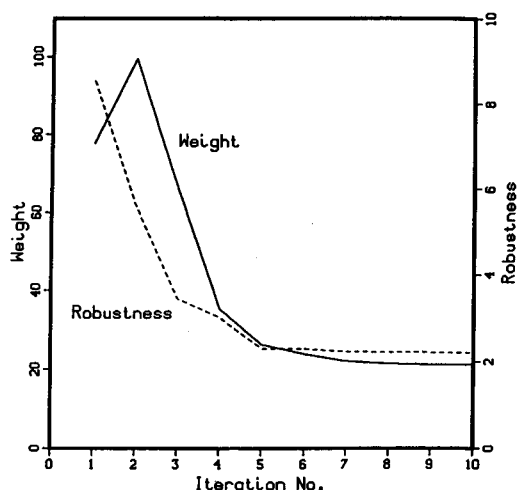


Fig. 9 ACOSS-FOUR design iteration history.

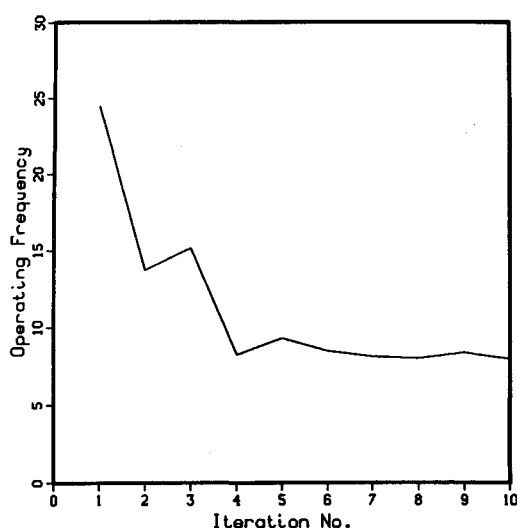


Fig. 10 ACOSS-FOUR operating frequency vs iterations.

weight rapidly increased with a larger improvement in the stability margin.

ACOSS-FOUR Model

The finite element model of ACOSS-FOUR is shown in Fig. 4. The structure has 12 degrees of freedom and four masses of two units each at nodes 1-4. The cross-sectional areas of the members for the initial design were equal to those assigned by the Charles Stark Draper Laboratory model.² Similar to the preceding example, first the structure was designed without a robustness constraint. The numerical studies were performed by imposing the design requirements $\bar{\omega}_1 \geq 1.341$, $\bar{\omega}_2 \geq 1.6$, and $\xi_1 \geq 0.15$. The lower bound on the design variables was 10 units. The structural weight decreased from 43.70 to 18.56 units. At this design the robustness bound is 1.69. In case II.2 in Table 2, a lower limit on robustness was imposed to improve the bound by 10%. The optimization was carried out by keeping the preceding three constraints. The optimum design was realized with a 4% increase in the objective function. Table 2 provides the optimum weight, constraints, and design variables, and also has case II.3 results where the bound was increased by 30%. Figure 9 shows the structural weight and robustness bound iteration histories for case II.3. The changes in critical operating frequency with the progress of optimization are shown in Fig. 10. As the optimum design is approached, p value reaches a steady value. This suggests that additional savings can be realized in computing the robustness bound after five to six iterations of optimization. The critical

operating frequency value can be kept constant and, thus, several matrix inversion and complex eigenvalue calculations can be reduced in finding the guaranteed robustness bound.

To calculate the total performance index J and the control effort, a unit displacement was imposed at node 2 in the X direction at time $t = 0$. The transient response was simulated by finding the solution to Eq. (4) for the period $t = 0$ to 25 s. The total performance index J and the work done by all the actuators is given in Table 3. Total actuators work is computed by summing the $\int f_i \dot{u}_i(t) dt$ for each actuator during the 25 s. period. Here, f_i is the i th actuator force and \dot{u}_i is the i th velocity component. Table 3 also gives the minimum and maximum values of the closed-loop damping parameters and the imaginary part of the eigenvalues for all cases. The range of the closed-loop eigenvalues and the magnitude of damping values increased with an increase in the robustness. The total performance index and the control effort also increased.

Summary

In this work, a robustness bound was defined for improving the stability margins of the closed-loop system due to parametric uncertainties. Based on the example problems considered in this work, the laborious computations involved in calculating the robustness measure were reduced by identifying the relationship between the spectral radius peaks locations and the closed-loop eigenvalue magnitudes. Structural examples were given with and without the robustness requirement. Stability margins improvement occurs at the cost of additional structural weight. The relationship between the stability robustness and the optimum structural weight is nonlinear as demonstrated by the example cases.

Acknowledgment

This research work was supported by the U.S. Air Force through Contract F33615-88-C-3204.

References

- Haftka, R. T., Martinovic, Z., and Hallauer, W. L., Jr., "Enhanced Vibration Controllability by Minor Structural Modifications," *AIAA Journal*, Vol. 23, No. 8, 1985, pp. 1260-1266.
- Khot, N. S., "Structures/Control Optimization to Improve the Dynamic Response of Space Structures," *Journal of Computational Mechanics*, Vol. 3, 1988, pp. 179-186.
- Lust, R. V., and Schmit, L. A., "Control Augmented Structural Synthesis," *AIAA Journal*, Vol. 26, No. 1, 1988, pp. 86-95.
- Rao, S. S., Venkayya, V. B., and Khot, N. S., "Game Theory Approach for the Integrated Design of Structures and Controls," *AIAA Journal*, Vol. 26, No. 4, 1988, pp. 463-469.
- Thomas, H. L., and Schmit, L. A., Jr., "Control Augmented Structural Synthesis with Dynamic Stability Constraints," *Proceedings of the AIAA/ASME/ASCE/AHS/ASC 30th Structures, Structural Dynamics and Materials Conference*, Part 1, AIAA, Washington, DC, 1989, pp. 521-531.
- Grandhi, R. V., "Structural and Control Optimization of Space Structures," *International Journal of Computers & Structures*, Vol. 31, No. 2, 1989, pp. 139-150.
- Patel, R. V., Toda, M., and Sridhar, B., "Robustness of Linear Quadratic State Feedback Designs in the Presence of System Uncertainty," *IEEE Transactions on Automatic Control*, Vol. 22, Dec. 1977, pp. 945-949.
- Patel, R. V., and Toda, M., "Quantitative Measures of Robustness for Multivariable Systems," *Proceedings of the Joint Automatic Control Conference*, San Francisco, TP8-A, 1980.
- Yedavalli, R. K., "Improved Measures of Stability Robustness for Linear State-space Models," *IEEE Transactions on Automatic Control*, Vol. 30, June 1985, pp. 577-579.
- Yedavalli, R. K., Banda, S. S., and Ridgely, D. B., "Time Domain Stability Robustness Measures for Linear Regulators," *Journal of Guidance, Control, and Dynamics*, Vol. 8, No. 4, 1985, pp. 520-525.
- Juang, Y., Kuo, T., and Hsu, C., "New Approach to Time-Domain Analysis for Stability Robustness of Dynamic Systems," *International Journal of Systems Science*, Vol. 18, No. 7, 1987, pp. 1363-1376.

¹²Qiu, L., and Davison, E. J., "New Perturbation Bounds for the Robust Stability of Linear State Space Models," *Proceedings of the 25th Conference on Decision and Control*, Athens, Greece, 1986, pp. 751-755.

¹³Lim, K. B., and Junkins, J. L., "Robustness Optimization of Structural and Control Parameters," *Journal of Guidance, Control, and Dynamics*, Vol. 12, No. 1, 1989, pp. 89-96.

¹⁴Rew, D. W., Junkins, J. L., and Juang, J. N., "Robust Eigenstructure Assignment by a Projection Method: Applications using Multiple Optimization Criteria," *Journal of Guidance, Control, and Dynamics*, Vol. 12, No. 3, pp. 396-403.

¹⁵Juang, J., Lim, K. B., and Junkins, J. L., "Robust Eigensystem Assignment for Flexible Structures," *Journal of Guidance, Control, and Dynamics*, Vol. 12, No. 3, 1989, pp. 381-387.

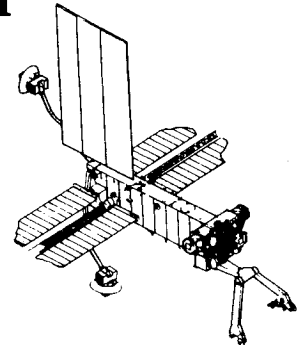
¹⁶Haq, I., Grandhi, R. V., and Yedavalli, R. K., "Robustness Measures for Integrated Structural/Control Systems," *Journal of Computing Systems in Engineering*, Vol. 1, Nos. 2-4, 1990, pp. 285-292.

¹⁷Grandhi, R. V., Thareja, R., and Haftka, R. T., "NEWSUMT-A: A General Purpose Program for Constrained Optimization Using Constraint Approximations," *ASME Journal of Mechanisms, Transmissions, and Automation in Design*, Vol. 107, March 1985, pp. 94-99.



Space Stations and Space Platforms—Concepts, Design, Infrastructure, and Uses

Ivan Bekey and Daniel Herman, editors



This book outlines the history of the quest for a permanent habitat in space; describes present thinking of the relationship between the Space Stations, space platforms, and the overall space program; and treats a number of resultant possibilities about the future of the space program. It covers design concepts as a means of stimulating innovative thinking about space stations and their utilization on the part of scientists, engineers, and students.

To Order, Write, Phone, or FAX:



American Institute of Aeronautics and Astronautics
c/o TASC0
9 Jay Gould Ct., P.O. Box 753, Waldorf, MD 20604
Phone (301) 645-5643 Dept. 415 FAX (301) 843-0159

1986 392 pp., illus. Hardback
ISBN 0-930403-01-0 Nonmembers \$69.95
Order Number: V-99 AIAA Members \$43.95

Postage and handling fee \$4.50. Sales tax: CA residents add 7%, DC residents add 6%. Orders under \$50 must be prepaid. Foreign orders must be prepaid. Please allow 4-6 weeks for delivery. Prices are subject to change without notice.